U.S. Department of Energy
National Energy Technology Laboratory

Enhanced Simulation Tools to Improve Predictions and Performance of Geologic Storage: Coupled Modeling of Fault Poromechanics, and High-Resolution Simulation of CO2 Migration and Trapping

Final Scientific Report

Original Period of Performance: October 1, 2012 – September 30, 2015
No-cost Extension: October 1, 2015 – September 30, 2016

Principal Investigator: Prof. Ruben Juanes
Tel: (617)253-7191
Email: juanes@mit.edu

Grant Award Number DE-FE0009738

Submitting Organization:
Massachusetts Institute of Technology
77 Massachusetts Avenue, Cambridge, MA 02139

December 31, 2016

Abstract

The main objective of this project was to develop tools for better understanding, modeling and risk assessment of CO2 permanence in geologic formations. Essential aspects include fault leakage, triggered fault slip and induced seismicity, and the effects of heterogeneity on CO2 migration. All of these must be addressed to safely inject CO2 at the gigatonne-per-year injection rate required to have an impact in the abatement of CO2 emissions. The specific objectives were:

1. To develop computational models that will enable assessing the potential for fault slip, leakage, and induced seismicity.

2. To develop computational methods for better predictions of capillary and solubility trapping at large scales and in the presence of aquifer heterogeneity.

3. To apply the models of fault poromechanics and CO2 migration and trapping to synthetic and actual deep saline aquifers.

We have developed a coupled model of flow and geomechanics of CO2 injection in deep geologic formations that is capable of simulating the poromechanics of faults, to assess the potential for fault slip and fault activation upon CO2 injection. We have used the fixed-stress sequential split of the coupled flowgeomechanics problem to develop an accurate, stable and efficient computational tool for simulating fault poromechanics. We did so by coupling a multiphase/compositional flow code with a geomechanics code capable of simulating static and dynamic geodeformation problems with localized deformation along faults. We implemented alternative descriptions of the dependence of the coefficient of friction on slip rate and state, and applied the code to synthetic and actual reservoirs to evaluate the risk of induced seismicity from CO2 storage. Finally, we developed high-resolution simulation tools to investigate the interplay between CO2-plume migration and CO2 trapping. The multidimensional models capture a wide range of scales from those associated with the convective dissolution instability (meters) to those related to the large-scale (tens of kilometers), to elucidate the impact of aquifer heterogeneity on CO2 migration and trapping.

The project has offered opportunities for training of *four PhD students* in the project. It has also led to over *20 peer-reviewed journal publications*, 4 conference papers, and many invited talks (including several plenary talks at international conferences) and seminars.

Overall, we believe that the current project is having a significant impact on society, and has the potential to have much more in the future, as a result of the development of quantitative numerical models of induced seismicity, a topic that has attracted the attention of society at large, especially in connection with waste water disposal from oil and gas production in the United States, as well as the potential for being a constraint for the implementation of carbon capture and storage at large scale.

Contents

1 Executive summary

Objectives. The main objective of this project was to develop tools for better understanding, modeling and risk assessment of CO2 permanence in geologic formations. Essential aspects include fault leakage, triggered fault slip and induced seismicity, and the effects of heterogeneity on CO2 migration. All of these must be addressed to safely inject CO2 at the gigatonne-per-year injection rate required to have an impact in the abatement of CO2 emissions. The specific objectives were:

1. To develop computational models that will enable assessing the potential for fault slip, leakage, and induced seismicity.

2. To develop computational methods for better predictions of capillary and solubility trapping at large scales and in the presence of aquifer heterogeneity.

3. To apply the models of fault poromechanics and CO2 migration and trapping to synthetic and actual deep saline aquifers.

The project has contributed to the advancement of fundamental science for deployment of CCS, and to training the next generation of scientists and engineers.

Methods. We have developed a coupled model of flow and geomechanics of CO2 injection in deep geologic formations that is capable of simulating the poromechanics of faults, to assess the potential for fault slip and fault activation upon CO2 injection. We have used the fixed-stress sequential split of the coupled flowgeomechanics problem to develop an accurate, stable and efficient computational tool for simulating fault poromechanics. We did so by coupling a multiphase/compositional flow code with a geomechanics code capable of simulating static and dynamic geodeformation problems with localized deformation along faults. We implemented alternative descriptions of the dependence of the coefficient of friction on slip rate and state, and applied the code to synthetic and actual reservoirs to evaluate the risk of induced seismicity from CO2 storage. Finally, we developed high-resolution simulation tools to investigate the interplay between CO2-plume migration and CO2 trapping. The multidimensional models capture a wide range of scales from those associated with the convective dissolution instability (meters) to those related to the large-scale (tens of kilometers), to elucidate the impact of aquifer heterogeneity on CO2 migration and trapping.

Outcomes. The project has offered opportunities for training of *four PhD students* in the project, Birendra Jha, Xiaojing Fu, Benzhong Zhao, and Yuval Tal.

It has also led to over *20 peer-reviewed journal publications*, 4 conference papers, and many invited talks (including several plenary talks at international conferences) and seminars.

The project has also led to important scientific collaborations, including: (1) a continuing interaction with the USGS Menlo Park office; (2) discussions with Dr. Brad Aagaard, who is one of the main developers of the PyLith software used on this project and is implementing improvements to the rate-state algorithm that we have suggested are needed based on our research; (3) a collaboration with Dr. Christopher MacMinn at University of Oxford and Dr. Juan Hidalgo at the Spanish National Research Council on the simulation of CO_2 migration and dissolution; (4) a

collaboration with Dr. Anna Scotti from the Politechnic Institute of Milan on mathematical formulations for flow along discrete faults; (5) a collaboration with a team of world experts in the area of induced seismicity, which includes: Prof. John H. Shaw and Dr. Andreas Plesch (Harvard University), Prof. James H. Dieterich (University of California Riverside), and Dr. Cliff Frohlich (University of Texas Austin).

Impact. The outcomes from the project are having a definitive impact on the field of computational modeling of coupled flow and geomechanics, especially as applied to geologic CO2 sequestration. Our paper (Jha and Juanes, *Water Resour. Res.* 2014) is arguably becoming a *de facto* reference in the field, and the computational approach developed in this project is now being pursued by other research groups, including Lawrence Livermore and Lawrence Berkeley National Labs. The project is having a direct impact in the field of oil and gas recovery, especially as it relates to the potential impact of reservoir operations on induced seismicity. The technology and know-how developed as part of this project are now being recognized by industry and governments by commissioning studies to assess the impact of water injection or gas injection on recorded seismicity. The project has already served as a catalyst for complementary industry-funded projects that focus on the critical issue of better understanding potential leakage associated with fault slip.

Overall, we believe that the current project is having a significant impact on society, and has the potential to have much more in the future, as a result of the development of quantitative numerical models of induced seismicity, a topic that has attracted the attention of society at large, especially in connection with waste water disposal from oil and gas production in the United States, as well as the potential for being a constraint for the implementation of carbon capture and storage at large scale.

Project benefits. In this project we conducted research under Area of Interest 4 of the original Funding Opportunity Announcement: Enhanced Simulation Tools to Improve Predictions and Enhance Performance of Geologic Storage; New simulation approaches for simplified reservoir models to predict the extent of CO2 plume migration, brine movement, and pressure impact; and, Advanced simulation tools to assess and control natural system failures (faults, fractures, other discontinuities, caprock) and phenomena (brine migration) to predict and mitigate ground movement at faults and for water management to predict and control pressure. The project has advanced the current baseline technology by developing improved simulation approaches that incorporate heterogeneity and by developing a fully coupled flow–geomechanics software package that explicitly includes faults with realistic rheologies. The project supports the Carbon Storage Programs Goals to develop technologies to estimate storage capacity and to improve storage efficiency making substantial advances in understanding and documenting the important effects of heterogeneity. It supports the Goal of development of Best Practices Manuals, and contribute to the Goal of demonstrating 99% storage permanence, by providing advanced simulation tools to understand and predict fault motion, fault transmissivity, and induced seismicity.

2 Organization of the report

In this project we developed a coupled model of ow and geomechanics of CO2 injection in deep geologic formations that is capable of simulating the poromechanics of faults, with the objective of assessing the potential for fault slip and fault activation upon CO2 injection. We employ the fixed-stress sequential split of the coupled ow–geomechanics problem to develop an accurate, stable and efficient computational tool for simulating fault poromechanics. This has been completed by coupling a multiphase/compositional flow code with a geomechanics code capable of simulating static and dynamic geodeformation problems allowing for localized deformation along faults.

This coupled modeling tool will be used to study the risk of triggered fault slip and induced seismicity. Alternative descriptions of the dependence of the coefficient of friction on slip rate and state have been developed and implemented, and the code was applied to synthetic and actual formations to evaluate the risk of induced seismicity from CO2 storage.

Finally, high-resolution simulation tools were developed to investigate the interplay between CO2-plume migration and CO2 trapping. The multidimensional models capture a wide range of scales from those associated with the convective dissolution instability (meters) to those related to the large-scale (tens of kilometers), and allows for better understanding of the impact of formation heterogeneity on CO2 migration and trapping.

The report is organized following the three main thrusts of the original proposal:

1. Coupled modeling of flow and fault geomechanics.

2. Investigation of effects of fault rheology, pre-existing stress, and fluid pressure changes on triggered fault slip and induced seismicity.

3. High-resolution simulation of CO2 migration and trapping.

3 Coupled modeling of flow and fault geomechanics

3.1 Coupled multiphase flow and poromechanics: a computational model of pore-pressure effects on fault slip and earthquake triggering [8, 9]

The coupling between subsurface flow and geomechanical deformation is critical in the assessment of the environmental impacts of groundwater use, underground liquid waste disposal, geologic storage of carbon dioxide , and exploitation of shale gas reserves. In particular, seismicity induced by fluid injection and withdrawal has emerged as a central element of the scientific discussion around subsurface technologies that tap into water and energy resources. Here, we present a new computational approach to model coupled multiphase flow and geomechanics of faulted reservoirs. We represent faults as surfaces embedded in a three-dimensional medium by using zero-thickness interface elements to accurately model fault slip under dynamically evolving fluid pressure and fault strength. We incorporate the effect of fluid pressures from multiphase flow in the mechanical stability of faults, and employ a rigorous formulation of nonlinear multiphase geomechanics that is capable of handling strong capillary effects. We develop a numerical simulation tool by coupling a multiphase flow simulator with a mechanics simulator, using the unconditionally stable fixed-stress scheme for the sequential solution of two-way coupling between flow and geomechanics. We validate our modeling approach using several synthetic, but realistic, test cases that illustrate the onset and evolution of earthquakes from fluid injection. (Figs. 1 and 2).

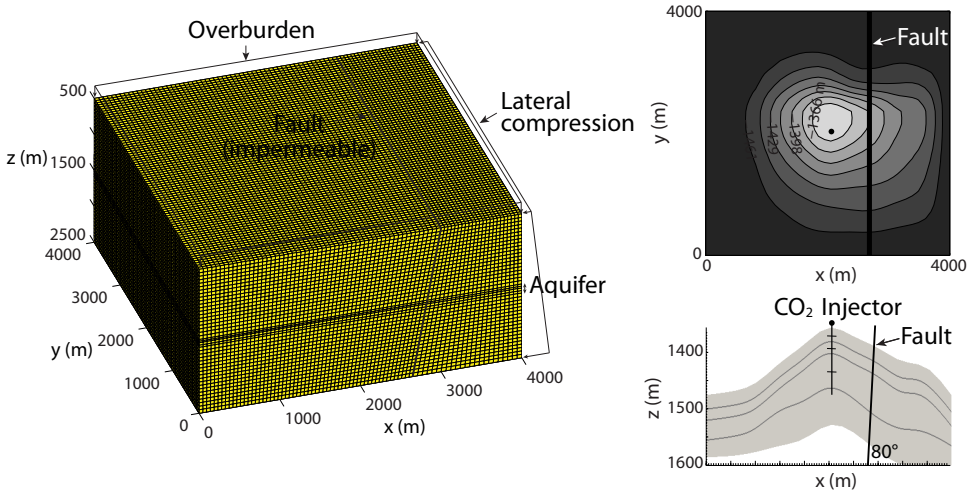

Figure 1. CO_2 injection in a 3D anticlinal aquifer. Left: the geomechanical domain, shown with the traction boundary conditions on the top and on the right boundaries. The lateral compression is 0.7 times the overburden, and both increase with the lithostatic gradient. Zero normal displacement is imposed on all other boundaries. A no-flow boundary condition is imposed on all the boundaries. The flow domain is composed of the four layers marked as *aquifer*, and the injector is located near the center of the anticline. Right: plan view (top figure) and cross-section view (bottom figure) of the aquifer. Depth contours are marked in the plan view. The cross-section view is exaggerated in the vertical direction.

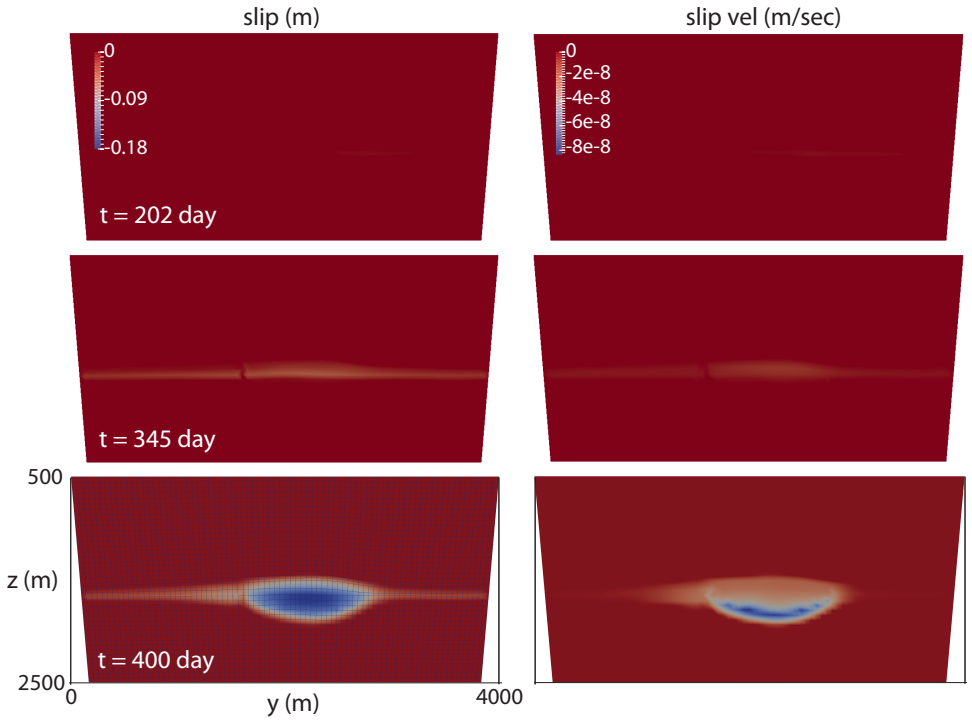

Figure 2. CO_2 injection in a 3D anticlinal aquifer. Snapshots of slip magnitude (left) and slip velocity (right) on the fault plane at three different times: $t = 202$, 345 and 400 day. The rupture initiates at the bottom of the aquifer and progresses both downwards and upwards with faster slip velocity downwards. The rupture front adopts an ellipsoidal shape following the profile of the aquifer, which is being pressurized.

3.2 Rigorous coupling of geomechanics and multiphase flow with strong capillarity [13]

We study sequential formulations for coupled multiphase flow and reservoir geomechanics. First, we identify the proper definition of effective stress in multiphase-fluid systems. Although the average pore pressure $\bar{p}$—defined as the sum of the product of saturation and pressure of all the fluid phases that occupy the pore space—is commonly used to describe multiphase-fluid flow in deformable porous media, it can be shown that the "equivalent" pore-pressure p_E—defined as $\bar{p}$ minus the interfacial energy—is the appropriate quantity (Coussy, *Poromechanics*, 2004). We show, by means of a fully implicit analysis of the system, that only the equivalent pore pressure p_E leads to a continuum problem that is thermodynamically stable (thus, numerical discretizations on the basis of the average pore pressure $\bar{p}$ cannot render unconditionally stable and convergent schemes). We then study the convergence and stability properties of sequential-implicit coupling strategies. We show that the stability and convergence properties of sequential-implicit coupling strategies for single-phase flow carry over for multiphase systems if the equivalent pore pressure p_E is used. Specifically, the undrained and fixed-stress schemes are unconditionally stable, and the fixed-stress split (FSS) is superior to the undrained approach in terms of convergence rate. The findings from stability theory are verified by use of nonlinear simulations of two-phase flow in deformable reservoirs.

3.3 Reservoir characterization in an underground gas storage field using joint inversion of flow and geodetic data [10]

Characterization of reservoir properties like porosity and permeability in reservoir models typically relies on history matching of production data, well pressure data, and possibly other fluid-dynamical data. Calibrated (history-matched) reservoir models are then used for forecasting production, and designing effective strategies for improved oil and gas recovery. Here, we perform assimilation of both flow and deformation data for joint inversion of reservoir properties. Given the coupled nature of subsurface flow and deformation processes, joint inversion requires efficient simulation tools of coupled reservoir flow and mechanical deformation. We apply our coupled simulation tool to a real underground gas storage field in Italy (Fig. 3). We simulate the initial gas production period, and several decades of seasonal natural gas storage and production. We perform a probabilistic estimation of rock properties by joint inversion of ground deformation data from geodetic measurements and fluid flow data from wells. Using an efficient implementation of the Ensemble Smoother as the estimator, and our coupled multiphase flow and geomechanics simulator as the forward model, we show that incorporating deformation data leads to a significant reduction of uncertainty in the prior distributions of rock properties such as porosity, permeability, and pore compressibility.

3.4 Were the May 2012 Emilia–Romagna earthquakes induced? A coupled flow-geomechanics modeling assessment [12]

Seismicity induced by fluid injection and withdrawal has emerged as a central element of the scientific discussion around subsurface technologies that tap into water and energy resources. Here we

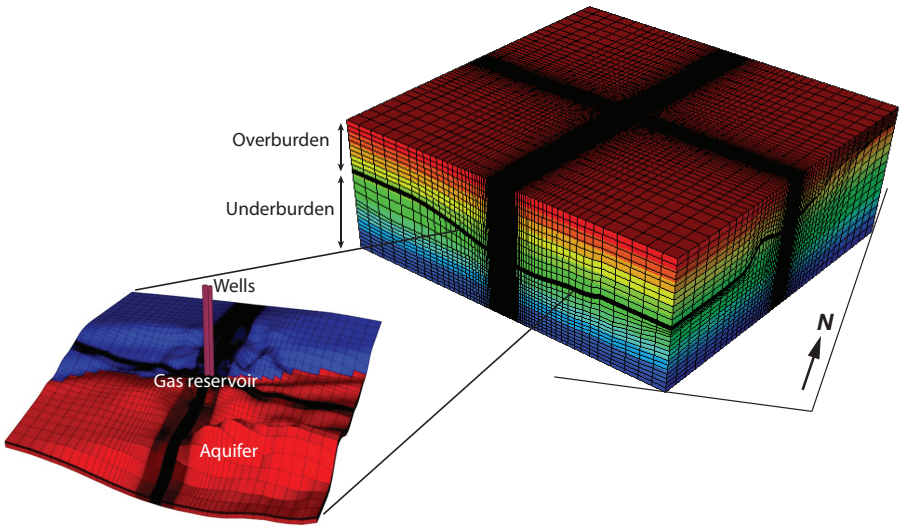

Figure 3. Geomechanical simulation grid (right) and a magnified view of the flow simulation grid (left). The grids are exaggerated by a factor of 7 in the vertical direction and axis labels are in unit of meter. The flow domain appears sandwiched between the overburden and the underburden. The flow domain has two parts, active and inactive, indicated by red and blue color, respectively. Fluid flow is assumed to occur only in the active part, which is composed of the gas reservoir and the aquifer. Wells are drilled into the gas reservoir.

present the application of coupled flow-geomechanics simulation technology to the post mortem analysis of a sequence of damaging earthquakes (Mw=6.0 and 5.8) in May 2012 near the Cavone oil field, in Northern Italy. This sequence raised the question of whether these earthquakes might have been triggered by activities due to oil and gas production. Our analysis strongly suggests that the combined effects of fluid production and injection from the Cavone field were not a driver for the observed seismicity (Fig. 4). More generally, our study illustrates that computational modeling of coupled flow and geomechanics permits the integration of geologic, seismotectonic, well log, fluid pressure and flow rate, and geodetic data, and provides a promising approach for assessing and managing hazards associated with induced seismicity.

3.5 Uncertainty quantification and inverse modeling of fault poromechanics and induced seismicity: application to a synthetic carbon capture and storage (CCS) problem [1]

Coupling between fluid flow and mechanical deformation in porous media plays a critical role in subsurface hydrology, oil and gas operations and seismic activity in the Earth's crust. For carbon capture and storage (CCS) projects, these coupled phenomena determine the interactions between the underground injection of CO2, the geomechanical properties of the reservoir and the stability of existing faults. As a result of the inherent uncertainty that is present in complex geological structures, assessing fault stability and the potential for induced seismicity is a fundamental challenge in any modeling effort for CCS projects. Here we present a formal framework for uncertainty analysis and data assimilation, which relies on a two-way-coupled computational modeling strategy for fluid flow and poromechanics of faults. We first quantify the sensitivity of key earthquake at-

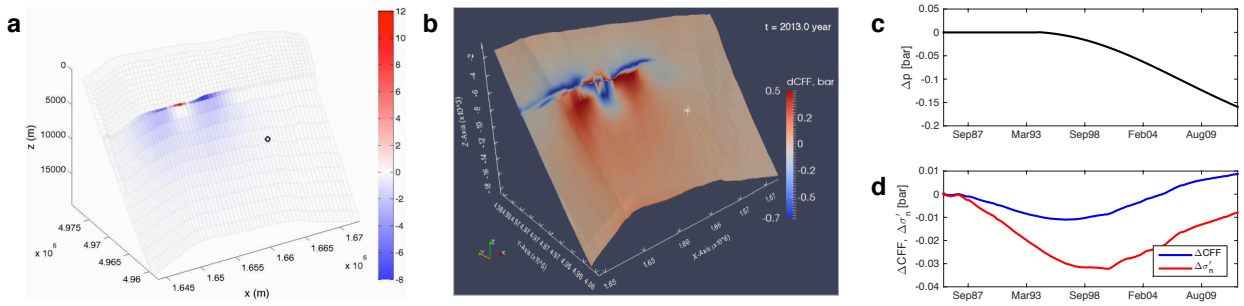

Figure 4. Results from the coupled flow-geomechanics dynamic model. (a) Pressure variation (in bar) at the hanging wall side of the Mirandola fault at the end of the simulation (31 December 2012). Red color indicates pressure buildup as a result of injection in the Cavone #14 well. Blue color indicates pressure decline as a result of fluid extraction, which extends into the underlying aquifer. The 29 May 2012 hypocenter location is shown with a circle. See Movie S1 in the supporting information for a video of the pressure-change evolution. (b) Changes in the Coulomb stress ΔCFF on the Mirandola fault (in bar) at the end of the simulation (31 December 2012). The change in the effective normal traction is positive near producers and negative near injectors because pressure depletion leads to contraction of the reservoir and pressure increase leads to increased compression on the fault. The white cross mark on the CFF plot denotes the hypocenter location of the 29 May 2012 earthquake. (c, d) Time evolution of changes in pressure and Coulomb stress (respectively) at the 29 May 2012 hypocenter location.

tributes (time of triggering, hypocenter location, and earthquake magnitude) to geologic properties such as rock permeability and coefficient of friction of the fault. We then perform a Bayesian inversion that combines Gaussian Processes with Markov Chain Monte Carlo (MCMC), from which we determine the posterior distribution of the system parameters. We show that this posterior distribution correctly combines information from the synthetic earthquake observations with a priori knowledge about the unknown parameters (Fig. 5).

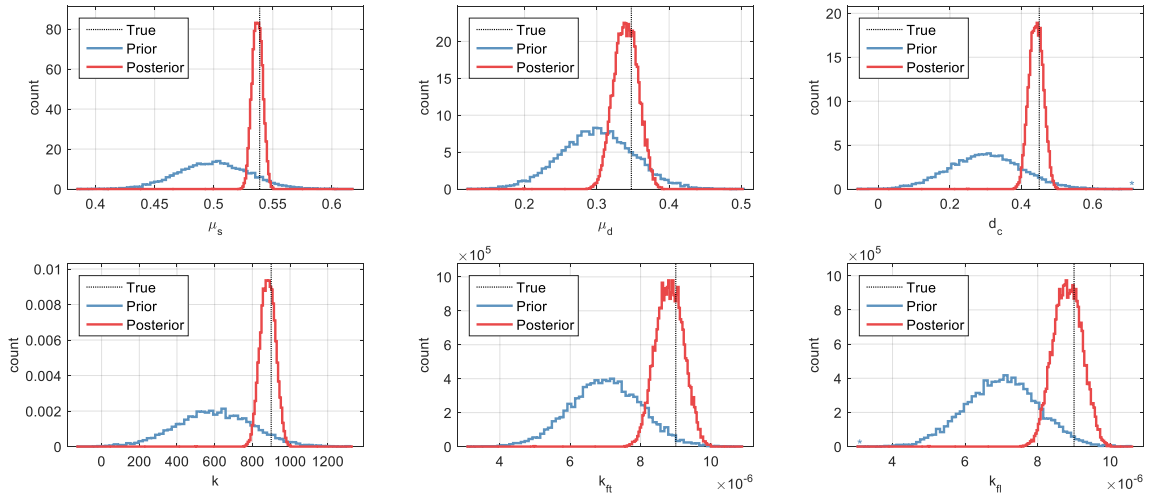

Figure 5. Posterior distributions using synthetic data from the "true" value of the parameters and observational noise, conditioning on earthquake attributes.

4 Investigation of effects of fault rheology, pre-existing stress, and fluid pressure changes on triggered fault slip and induced seismicity

4.1 An empirical study of the distribution of earthquakes with respect to rock type and depth [19]

Whether fault slip occurs seismically or aseismically depends on the frictional properties of the fault, which might be expected to depend on rock type and depth, as well as other factors. To examine the effect of rock type and depth on the distribution of earthquakes, we compare geologic models of the San Francisco Bay and the Southern California regions to the distribution of seismicity. We normalize the number of earthquakes within each rock type and depth interval by the corresponding volume to determine the earthquake density. Earthquake density is determined primarily by depth, while whether the rock is sedimentary or basement has only a secondary, depth-dependent effect on the earthquake density. At very shallow depths, there is no difference in earthquake density between sedimentary and basement rocks. The earthquake density of basement rocks increases with depth more rapidly than that of sedimentary rocks to a similar but shallower maximum (Fig. 6).

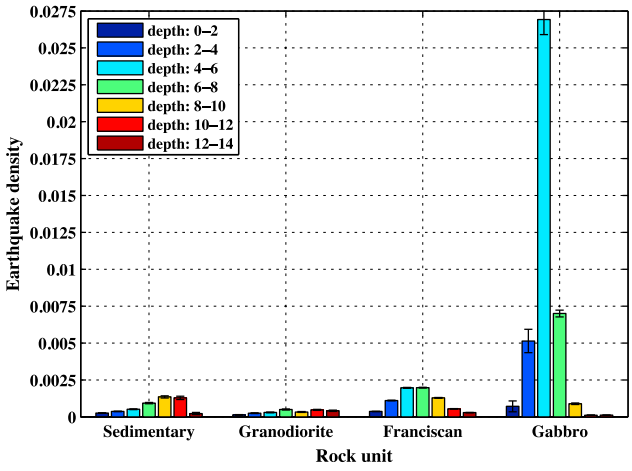

Figure 6. Earthquake density as a function of rock unit and depth in the San Francisco Bay region. The four main rock units at depths of 0–14 km are included. The error bars were derived from 5000 bootstraps and represent 1 standard error.

4.2 The two sides of a fault: grain-scale analysis of fault slip under discontinuous pore pressure [20]

Pore fluid pressure in a fault zone can be altered by natural processes (e.g., mineral dehydration and thermal pressurization) and industrial operations involving subsurface fluid injection/extraction for the development of energy and water resources. However, the effect of pore pressure change on the stability and slip motion of a preexisting geologic fault remains poorly understood; yet it is critical

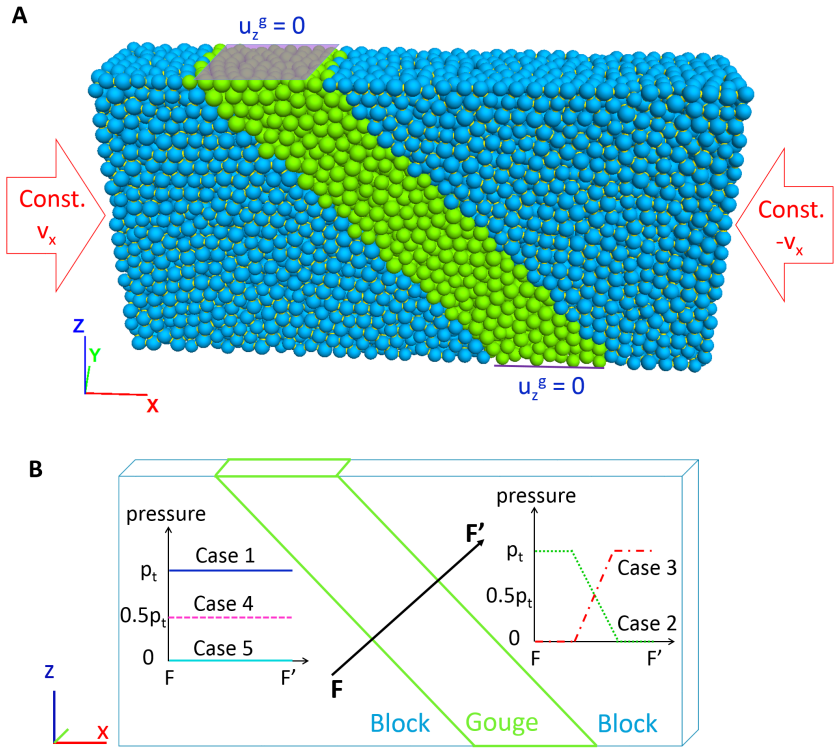

Figure 7. **A**, 3D block–gouge system composed of 7878 particles. The light green particles are unbonded, representing the gouge, while the blue particles are bonded, representing the blocks (fault walls). The origin of axes is placed at the center of the gouge layer. Rigid frictionless walls (not shown) are used to provide mechanical boundary conditions. Loading in the x direction with constant velocity drives the system to slip failure. The front and back walls are assigned zero displacement condition ($u_y = 0$). To reproduce relative motion with respect to the gouge layer, we impose zero vertical displacement at the top and bottom of the gouge layer ($u_z^g = 0$). **B**, Pore pressure cases. Cases 1, 4 and 5 represent continuous pressure across the fault, with Case 4 having a pressure half of that in Case 1, and Case 5 having zero pore pressure (dry system). Cases 2 and 3 represent discontinuous pressure across the fault, with a strong pressure gradient within the gouge layer.

for the assessment of seismic hazard. Here, we develop a micromechanical model to investigate the effect of pore pressure on fault slip behavior. The model couples fluid flow on the network of pores with mechanical deformation of the skeleton of solid grains. Pore fluid exerts pressure force onto the grains, the motion of which is solved using the discrete element method. We conceptualize the fault zone as a gouge layer sandwiched between two blocks. We study the fault stability in the presence of a pressure discontinuity across the gouge layer, and compare it with the case of continuous (homogeneous) pore pressure. We focus on the onset of shear failure in the gouge layer, and reproduce conditions where the failure plane is parallel to the fault (Fig. 7). We show that when the pressure is discontinuous, the onset of slip occurs on the side with the higher pore pressure, and that this onset is controlled by the maximum pressure on both sides of the fault. The results shed new light on the use of the effective stress principle and the Coulomb failure criterion in evaluating the stability of a complex fault zone. (Fig. 8).

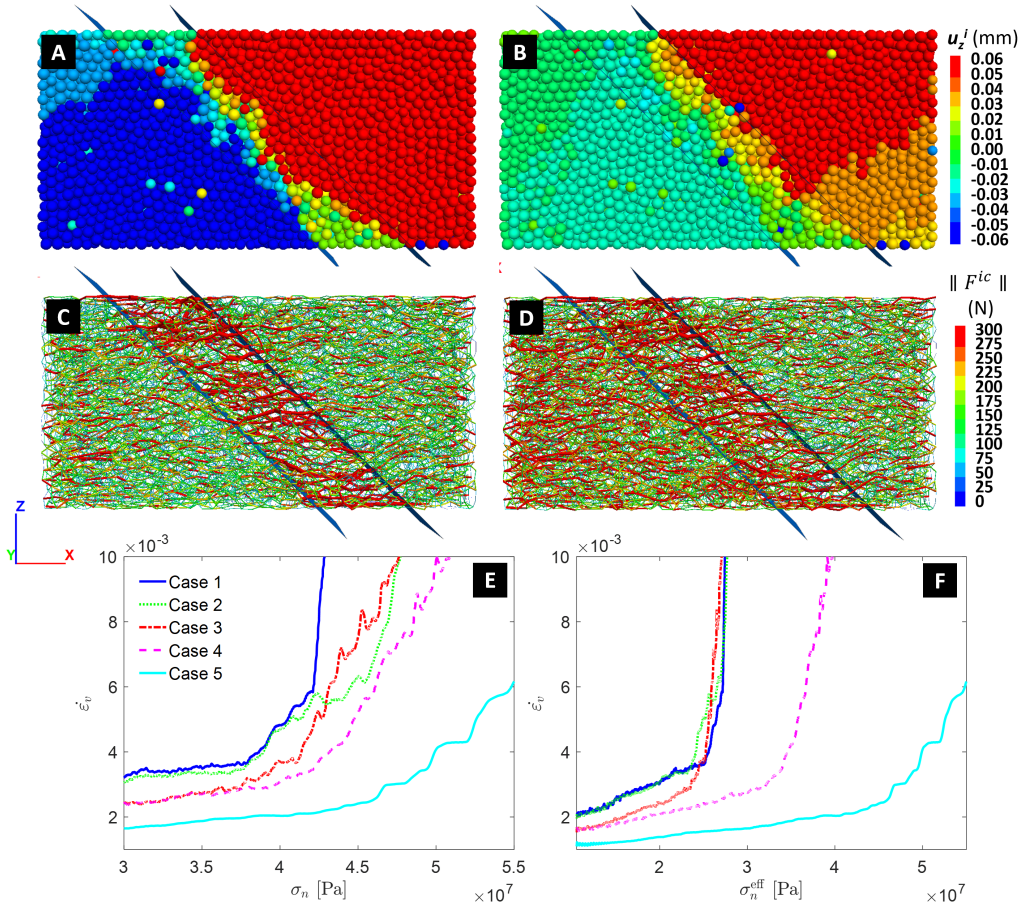

Figure 8. Slip behavior for the block–gouge system. **A, B**, Particle displacement in the z direction (A: pore pressure Case 1; B: Case 3; see Figure 7) at horizontal strain $\varepsilon_h = 3.1 \times 10^{-3}$. **C, D**, Contact force network with both color and link size representing force magnitude (C: pore pressure Case 1; D: Case 3) at horizontal strain $\varepsilon_h = 3.1 \times 10^{-3}$. **E**, Vertical strain rate [s^{-1}] as a function of normal stress in the fault gouge. **F**, Vertical strain rate [s^{-1}] as a function of *effective* normal stress $\sigma_n^{\text{eff}} = \sigma_n - p^f$ with fault pressure $p^f = \max(p^-, p^+)$.

5 High-resolution simulation of CO2 migration and trapping

5.1 Scaling of convective mixing in porous media [6]

Convective mixing in porous media is triggered by a Rayleigh–Bénard-type hydrodynamic instability as a result of an unstable density stratification of fluids (Fig. 9). While convective mixing has been studied extensively, the fundamental behavior of the dissolution flux and its dependence on the system parameters are not yet well understood. Here, we show that the dissolution flux and the rate of fluid mixing are determined by the mean scalar dissipation rate. We use this theoretical result to provide computational evidence that the classical model of convective mixing in porous media exhibits, in the regime of high Rayleigh number, a dissolution flux that is constant and independent of the Rayleigh number. Our findings support the universal character of convective mixing and point to the need for alternative explanations for nonlinear scalings of the dissolution flux with the Rayleigh number, recently observed experimentally.

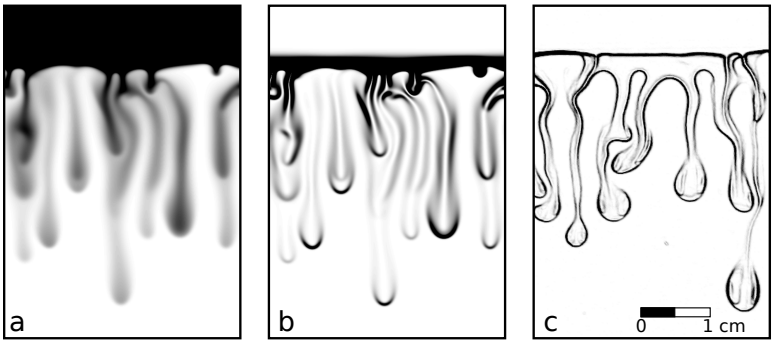

Figure 9. a, Snapshot of the concentration c at dimensionless time $t = 1$ from a simulation of the analogue-fluid system with Rayleigh number Ra $= 10,000$ and constant viscosity ($R = 0$). A computational grid of 512×1536 cells was used, and only a small window of the simulation domain is shown. **b,** Corresponding snapshot of the scalar dissipation rate ϵ, for the same simulation as that in figure a. Here, dark color corresponds to high values of ϵ, and indicates regions of active mixing. **c,** Snapshot of a surrogate of the scalar dissipation rate $\epsilon = \nabla c \cdot D_m \nabla c$ (obtained from light intensity) from a laboratory experiment with a PG–water system in a Hele-Shaw cell, illustrating that mixing is primarily confined to narrow layers along the edges of the horizontal interface and the density-driven fingers.

5.2 The evolution of miscible gravity currents in horizontal porous layers [15]

Gravity currents of miscible fluids in porous media are important to understand because they occur in important engineering projects, such as enhanced oil recovery and geologic CO_2 sequestration. These flows are often modeled based on two simplifying assumptions: vertical velocities are negligible compared to horizontal velocities, and diffusion is negligible compared to advection. In many cases, however, these assumptions limit the validity of the models to a finite, intermediate time interval during the flow, making prediction of the flow at early and late times difficult. Here, we consider the effects of vertical flow and diffusion to develop a set of models for the entire evolution of a miscible gravity current. To gain physical insight, we study a simple system: lock

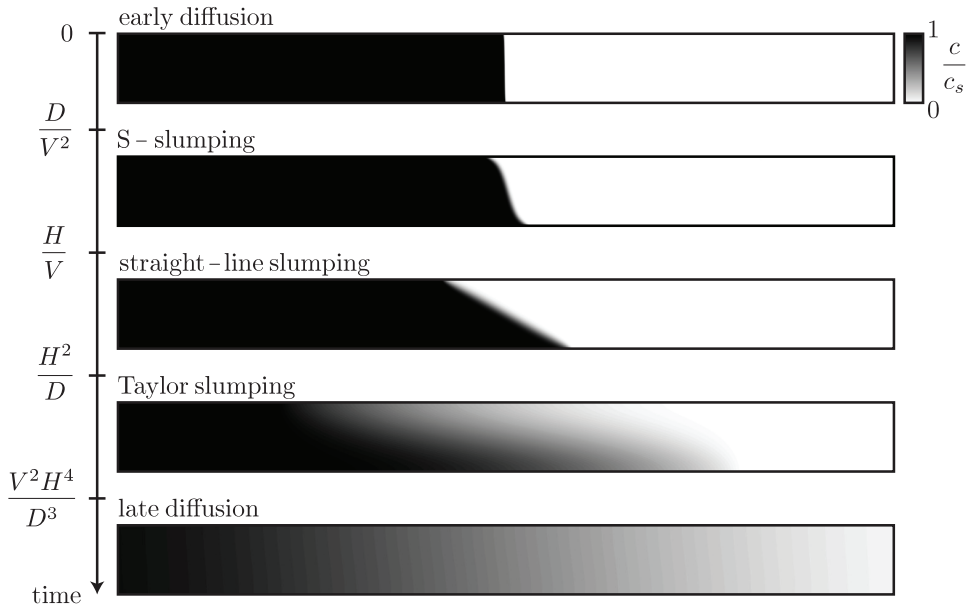

Figure 10. The flow evolves through the five self-similar regimes shown here by simulation results. The grey scale represents the concentration of the more dense fluid, c, normalized to the saturated concentration, c_s. The scalings of the transition times between the regimes are shown in terms of the layer thickness, H, the diffusion coefficient, D, and the characteristic velocity, $V = \Delta\rho g k/\mu\phi$. When $HV/D \lesssim 1$, the first and final transition times become equal, the duration of the intermediate regimes becomes zero, and lateral diffusion becomes the dominant mass transfer mechanism for all times.

exchange of equal-viscosity fluids in a horizontal, vertically-confined layer of permeable rock. We show that the flow exhibits five regimes: 1. an early-diffusion regime, in which the fluids diffuse across the initially sharp fluid-fluid interface; 2. an S-slumping regime, in which the fluid-fluid interface tilts in an S-shape; 3. a straight-line slumping regime, in which the fluid-fluid interface tilts as a straight line; 4. a Taylor-slumping regime, in which Taylor dispersion at the aquifer scale enhances mixing between the fluids and causes the flow to continuously decelerate; and 5. a late-diffusion regime, in which the flow becomes so slow that mass transfer again occurs dominantly though diffusion (Fig. 10).

5.3 Interface pinning of immiscible gravity-exchange flows in porous media [21]

We study the gravity-exchange flow of two immiscible fluids in a porous medium and show that, in contrast with the miscible case, a portion of the initial interface remains pinned at all times (Fig. 11). We elucidate, by means of micromodel experiments, the pore-level mechanism responsible for capillary pinning at the macroscale. We propose a sharp-interface gravity-current model that incorporates capillarity and quantitatively explains the experimental observations, including the $x \sim t^{1/2}$ spreading behavior at intermediate times and the fact that capillarity stops a finite-release current. Our theory and experiments suggest that capillary pinning is potentially an important, yet unexplored, trapping mechanism during CO_2 sequestration in deep saline aquifers (Fig. 12).

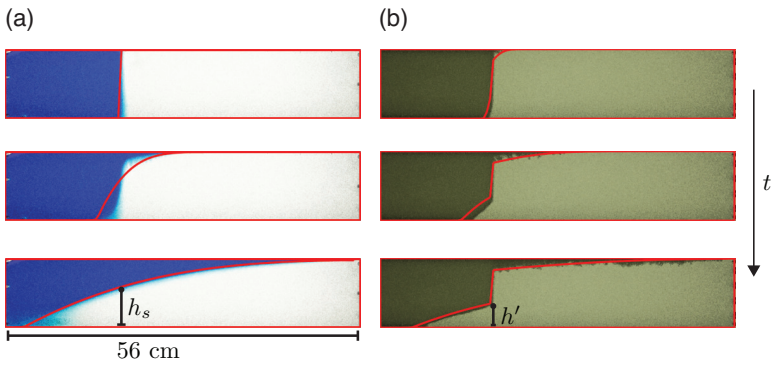

Figure 11. (Color online) Lock-exchange flow in a porous medium with (a) miscible and (b) immiscible fluids. (a) The miscible fluids are water (blue) spreading over a denser, more viscous mixture of glycerol and water. A smooth macroscopic interface tilts around a stationary point with fixed height h_s. (b) The immiscible fluids are air (dark) spreading over the same glycerol–water mixture. Part of the initial interface remains pinned, which leads to sharp kinks or "hinges" in the macroscopic interface. We denote the height of the lower hinge by h'. Both experiments were conducted in a transparent cell packed with 1 mm glass beads. The red curves correspond to the predictions of sharp-interface models.

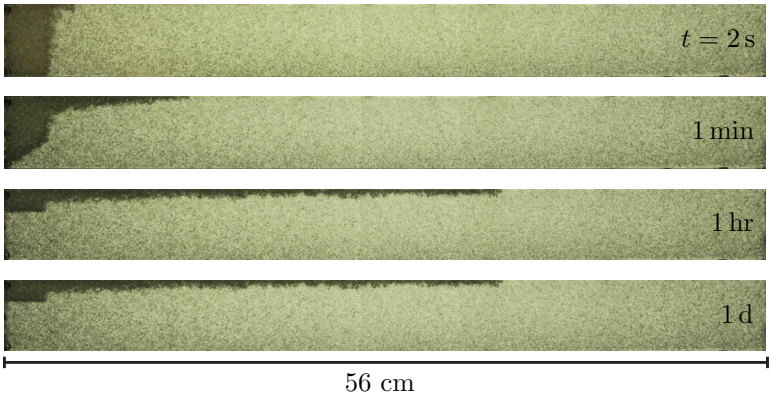

Figure 12. Finite release of a buoyant, nonwetting fluid (air) in a porous medium filled with a dense, wetting fluid (silicone oil). The dense, wetting front hits the left boundary, changing the spreading behavior of the buoyant current. Capillary hysteresis is responsible for the pinning of the initial interface and, ultimately, for stopping the buoyant plume at a finite distance, in stark contrast with a miscible plume which would continue to spread indefinitely.

5.4 Buoyant currents arrested by convective dissolution [14]

When carbon dioxide (CO_2) dissolves into water, the density of water increases. This seemingly insubstantial phenomenon has profound implications for geologic carbon sequestration. Here we show, by means of laboratory experiments with analogue fluids, that the up-slope migration of a buoyant current of CO_2 is arrested by the convective dissolution that ensues from a fingering instability at the moving CO_2–groundwater interface (Fig. 13). We consider the effectiveness of convective dissolution as a large-scale trapping mechanism in sloping aquifers, and we show that a small amount of slope is beneficial compared to the horizontal case. We study the development and coarsening of the fingering instability along the migrating current, and predict the maximum migration distance of the current with a simple sharp-interface model. We show that convective

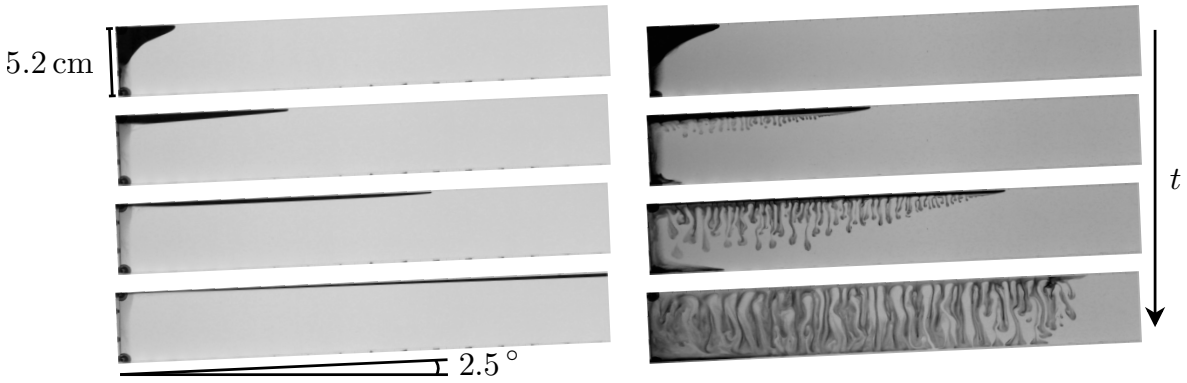

Figure 13. Convective dissolution arrests the up-slope migration of a buoyant current. Here we show snapshots of two buoyant currents migrating up-slope in a sloping aquifer (a Hele-Shaw cell for illustration). The CO_2 analogue is water (dark) in both cases. When the denser and more viscous ambient fluid is a mixture of glycerol and water (left), the fluids mix by diffusion-dispersion only and the buoyant current migrates to the top of the cell and accumulates there. When the ambient fluid is propylene glycol (right), the dense mixture of the two fluids drives convective dissolution, which dissolves the buoyant current as it migrates.

dissolution exerts a powerful control on CO_2 plume dynamics and, as a result, on the potential of geologic carbon sequestration.

5.5 Dynamics of convective dissolution from a migrating current of carbon dioxide [7]

During geologic storage of carbon dioxide (CO_2), trapping of the buoyant CO_2 after injection is essential in order to minimize the risk of leakage into shallower formations through a fracture or abandoned well. Models for the subsurface behavior of the CO_2 are useful for the design, implementation, and long-term monitoring of injection sites, but traditional reservoir-simulation tools are currently unable to resolve the impact of small-scale trapping processes on fluid flow at the scale of a geologic basin. Here, we study the impact of solubility trapping from convective dissolution on the up-dip migration of a buoyant gravity current in a sloping aquifer. To do so, we conduct high-resolution numerical simulations of the gravity current that forms from a pair of miscible analogue fluids. Our simulations fully resolve the dense, sinking fingers that drive the convective dissolution process (Fig. 14). We analyze the dynamics of the dissolution flux along the moving CO_2–brine interface, including its decay as dissolved buoyant fluid accumulates beneath the buoyant current. We show that the dynamics of the dissolution flux and the macroscopic features of the migrating current can be captured with an upscaled sharp-interface model.

5.6 Carbon dioxide dissolution in structural and stratigraphic traps [17]

The geologic sequestration of carbon dioxide (CO_2) in structural and stratigraphic traps is a viable option to reduce anthropogenic emissions. While dissolution of the CO_2 stored in these traps reduces the long-term leakage risk, the dissolution process remains poorly understood in systems that reflect the appropriate subsurface geometry. Here, we study dissolution in a porous layer that

Figure 14. Sequence of snapshots from a high-resolution simulation of convective dissolution from a buoyant current in a sloping aquifer for Ra $= 5000$, $R = 1$, and $\theta = 2.5°$ (not shown) at dimensionless times 0, 3, 9, and 27. The domain extends to $x = 20$, but only $0 \leq x \leq 15$ is shown here. The red line marks the contour of neutrally buoyant concentration $c = c_n$, which separates the buoyant current from the sinking fluid.

exhibits a feature relevant for CO_2 storage in structural and stratigraphic traps: a finite CO_2 source along the top boundary that extends only part way into the layer. This feature represents the finite extent of the interface between free-phase CO_2 pooled in a trap and the underlying brine. Using theory and simulations, we describe the dissolution mechanisms in this system for a wide range of times and Rayleigh numbers, and classify the behavior into seven regimes (Fig. 15). For each regime, we quantify the dissolution flux numerically and model it analytically, with the goal of providing simple expressions to estimate the dissolution rate in real systems. We find that, at late times, the dissolution flux decreases relative to early times as the flow of unsaturated water to the CO_2 source becomes constrained by a lateral exchange flow though the reservoir. Application of the models to several representative reservoirs indicates that dissolution is strongly affected by the reservoir properties; however, we find that reservoirs with high permeabilities ($k \geq 1$ Darcy) that are tens of meters thick and several kilometers wide could potentially dissolve hundreds of megatons of CO_2 in tens of years.

5.7 Capillary pinning and blunting of immiscible gravity currents in porous media [22]

Gravity-driven flows in the subsurface have attracted recent interest in the context of geological carbon dioxide (CO_2) storage, where supercritical CO_2 is captured from the flue gas of power plants and injected underground into deep saline aquifers. After injection, the CO_2 will spread and migrate as a buoyant gravity current relative to the denser, ambient brine. Although the CO_2 and the brine are immiscible, the impact of capillarity on CO_2 spreading and migration is poorly understood. We previously studied the early-time evolution of an immiscible gravity current, showing that capillary pressure hysteresis pins a portion of the macroscopic fluid-fluid interface and that this can eventually stop the flow. Here, we study the full lifetime of such a gravity current. Using tabletop experiments in packings of glass beads, we show that the horizontal extent of the pinned region grows with time, and that this is ultimately responsible for limiting the migration of the current to a

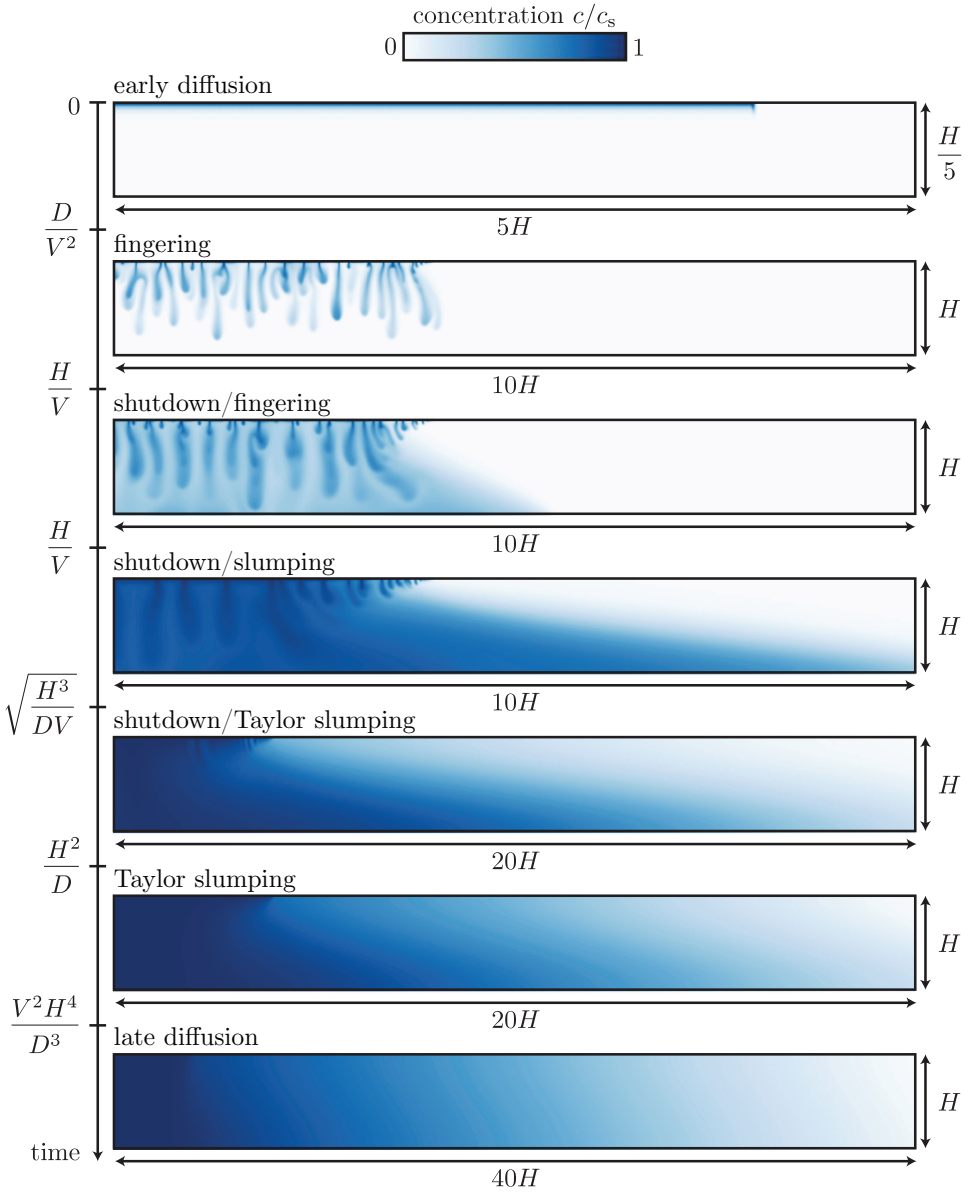

Figure 15. Dissolution evolves through the seven regimes shown here ($Ra = 3000$). The color scale represents the concentration of CO_2, c, normalized to the saturated concentration, c_s. The scalings of the transition times between the regimes are shown in terms of the layer thickness, H, the effective diffusion coefficient, D, and the characteristic velocity, $V = \Delta\rho g k/\mu\phi$. When $Ra = VH/D$ is sufficiently small, the first and final transition times become equal, the duration of the intermediate regimes becomes zero, and the system transitions directly to the late diffusion regime.

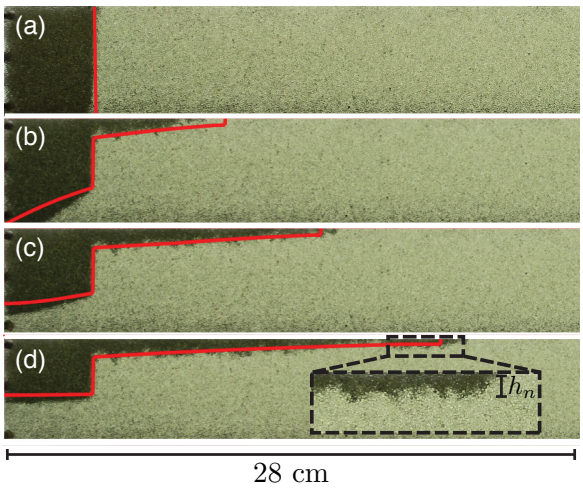

Figure 16. Gravity driven flow of a buoyant, nonwetting fluid (air) over a dense, wetting fluid (propylene glycol) in a packing of glass beads. (a-b) Starting with a vertical interface between the fluids, the flow first undergoes a lock-exchange process. (c-d) The process models a finite-release problem after the dense fluid reaches the left boundary. In contrast to the finite release of a miscible current that spreads indefinitely, spreading of an immiscible current stops at a finite distance. Dashed black box highlights the blunt nose of the current, which has thickness h_n. Red lines represent predictions from our macroscopic sharp-interface model.

finite distance (Fig. 16). We also find that capillarity blunts the leading edge of the current, which contributes to further limiting the migration distance. Using experiments in etched micromodels, we show that the thickness of the blunted nose is controlled by the distribution of pore-throat sizes and the strength of capillarity relative to buoyancy. We develop a theoretical model that captures the evolution of immiscible gravity currents and predicts the maximum migration distance. By applying this model to representative aquifers, we show that capillary pinning and blunting can exert an important control on gravity currents in the context of geological CO_2 storage.

5.8 Residual trapping, solubility trapping and capillary pinning complement each other to limit CO_2 migration in deep saline aquifers [23]

We derive a theoretical model for the post-injection migration of a CO_2 gravity current in a confined, sloping aquifer under the influence of residual trapping, solubility trapping, and capillary pinning. The resulting model consists of two coupled partial differential equations that describe the local thickness of the buoyant CO_2 current and the thickness of the mound of brine saturated with dissolved CO_2 as a function of time. We apply this model to a representative geological formation and provide estimates of the lifetime of the buoyant CO_2 current and its maximum migration distance. Our analysis shows that residual trapping, solubility trapping, and capillary pinning complement each other in limiting the ultimate migration distance of CO_2 gravity currents. The relative contribution of residual trapping, solubility trapping, and capillary pinning varies as a function of the injection volume. Our model can be used as a screening tool to evaluate the potential of deep saline aquifers for large-scale CO_2 sequestration.

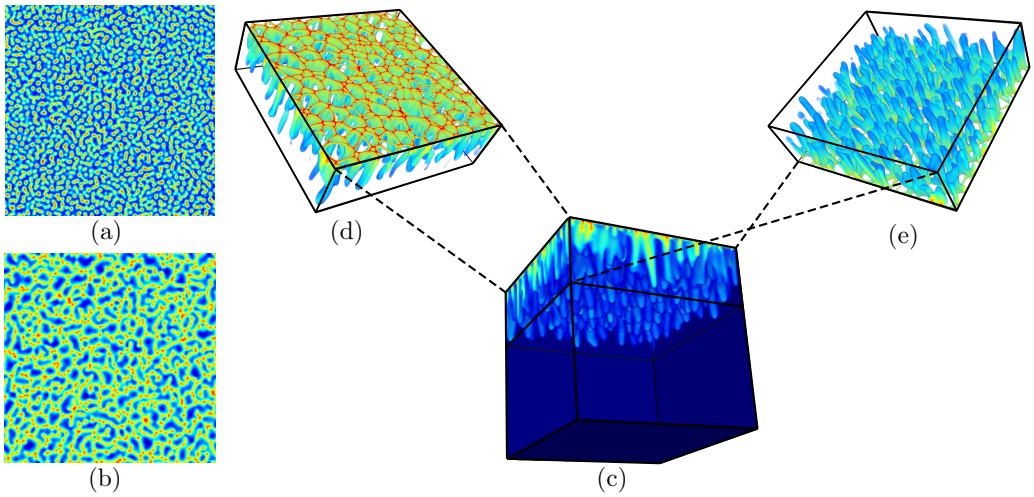

Figure 17. Simulation of convective mixing with Ra $= 6400$ on a 512^3 grid. (a) Snapshot of the concentration field at a slice near the top boundary ($z = 0.01$) at $t = 0.5$, showing a pattern of disconnected islands of high concentration. (b) Snapshot of the same slice at $t = 1$, showing a partially-connected maze structure. (c)-(e) Snapshot of the 3D concentration field at $t = 2$; (c) is a complete view of the computational domain; (d) is a view of a partial volume ($0.01 < z < 0.3$) from the top, illustrating the celular network structure that emerges at the boundary layer; (e) is a view of the same volume from the bottom, illustrating the columnar pattern of CO_2-rich fingers that sink away from the top boundary.

5.9 Pattern formation and coarsening dynamics in three-dimensional convective mixing in porous media [2]

Geologic carbon dioxide sequestration entails capturing and injecting CO_2 into deep saline aquifers for long-term storage. The injected CO_2 partially dissolves in groundwater to form a mixture that is denser than the initial groundwater. The local increase in density triggers a gravitational instability at the boundary layer that further develops into columnar plumes of CO_2-rich brine, a process that greatly accelerates solubility trapping of the CO_2. Here, we investigate the pattern-formation aspects of convective mixing during geological CO_2 sequestration by means of high-resolution three-dimensional simulation (Fig. 17). We find that the CO_2 concentration field self-organizes as a cellular network structure in the diffusive boundary layer at the top boundary. By studying the statistics of the cellular network, we identify various regimes of finger coarsening over time, the existence of a nonequilibrium stationary state, and a universal scaling of 3D convective mixing.

5.10 Theoretical analysis of how pressure buildup and CO_2 migration can both constrain storage capacity in deep saline aquifers [18]

Estimating the carbon dioxide (CO_2) storage capacity of deep saline aquifers is important for identifying those most suitable for sequestration, and for planning the future development of CO_2 storage projects. Currently, capacity estimates are highly uncertain due in part to uncertainty in the dominant constraint on capacity: both the pressure buildup from injection and the space available to trap CO_2 have been identified as constraints, but have not been rigorously compared to deter-

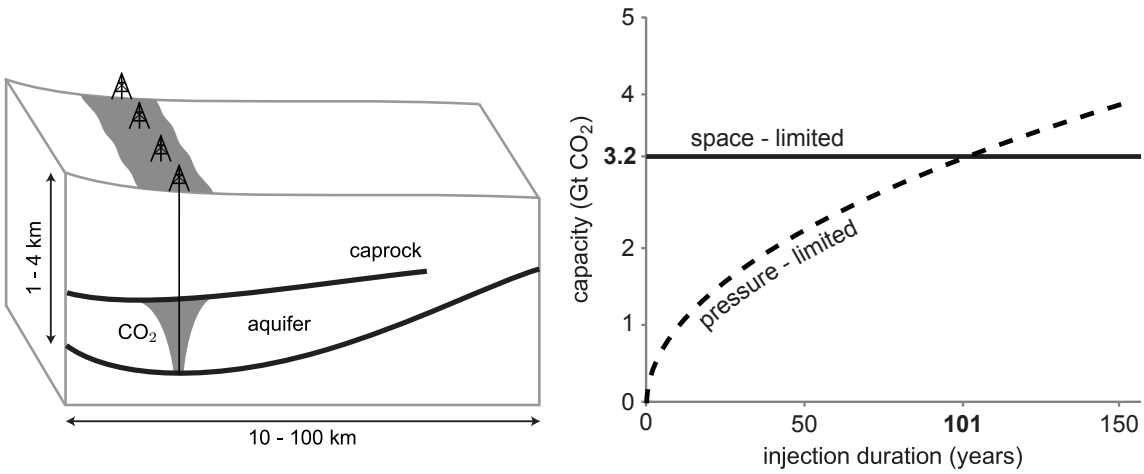

Figure 18. Left: We compare pressure and migration constraints on storage capacity in a model system: a deep saline aquifer at the basin scale, into which CO_2 is injected from a line-drive array of wells. Right: The pressure-limited capacity grows with the square root of injection time (dashed curve), but the migration-limited capacity is constant (solid curve). In the Fox Hills Sandstone, the capacity curves cross at an injection time of about 100 years, indicating that pressure constraints are more limiting for injection times less than 100 years, but migration constraints are more limiting for longer times.

mine the conditions under which each is more limiting. In this study, we evaluate their relative importance in an idealized aquifer using simple, but dynamic models of how pressure rises during injection and how CO_2 becomes trapped in the pore space (Fig. 18, left). We show that there exists a crossover time, T_c, below which pressure constraints dominate, but above which the CO_2 migration becomes the more limiting constraint. We illustrate this behavior by applying the models to the Fox Hills Sandstone (Fig. 18, right).

5.11 Rock dissolution patterns and geochemical shutdown of CO_2-brine-carbonate reactions during convective mixing in porous media [3]

Motivated by the process of CO_2 convective mixing in porous media, here we study the formation of rock-dissolution patterns that arise from geochemical reactions during Rayleigh–Bénard–Darcy convection. Under the assumption of instantaneous chemical equilibrium, we adopt a formulation of the local reaction rate as a function of scalar dissipation rate—a measure that depends solely on flow and transport—and chemical speciation, which is a measure that depends only on the equilibrium thermodynamics of the chemical system. We use high-resolution simulations to examine the interplay between the density-driven hydrodynamic instability and the rock dissolution reactions, and analyze the impact of geochemical reactions on the macroscopic mass exchange rate. We find that dissolution of carbonate rock initiates in regions of locally high mixing, but that the geochemical reaction shuts down significantly earlier than shutdown of convective mixing. This early shutdown feature reflects the important role that chemical speciation plays in this hydrodynamics–reaction coupled process. Finally, we extend our analysis to three dimensions and explore the morphology of dissolution patterns in 3D (Fig. 19).

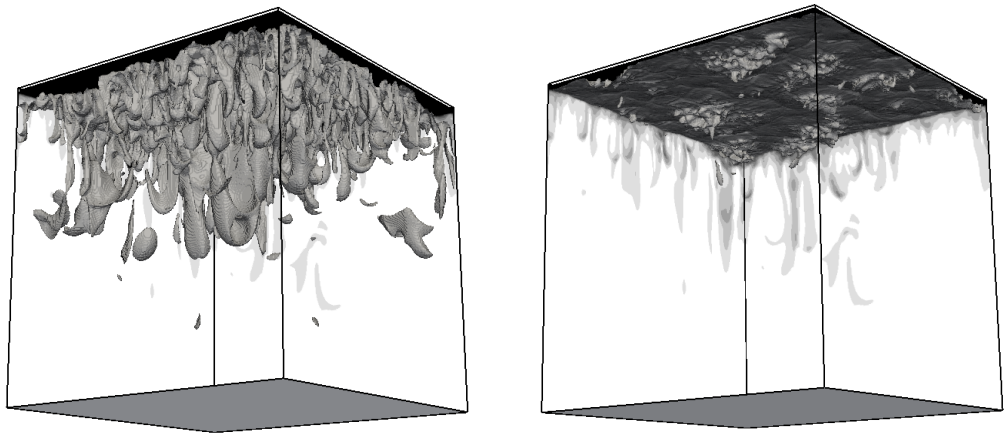

Figure 19. Rock dissolution patterns in 3D as a result of CO_2 convective mixing, for a simulation with H=2500, Da=5 and R_ϕ=2, at $t/H = 14.0$, this figure shows surface contours for (a) $\Delta\phi = 4\%$ and (b) $\Delta\phi = 8\%$.

5.12 Thermodynamic coarsening arrested by viscous fingering in partially-miscible binary mixtures [4]

We study the evolution of binary mixtures far from equilibrium, and show that the interplay between phase separation and hydrodynamic instability can arrest the Ostwald ripening process characteristic of non-flowing mixtures. We describe a model binary system in a Hele-Shaw cell using a phase-field approach with explicit dependence of both phase fraction and mass concentration. When the viscosity contrast between phases is large (as is the case for gas and liquid phases), an imposed background flow leads to viscous fingering, phase branching and pinch-off. This dynamic flow disorder limits phase growth and arrests thermodynamic coarsening. As a result, the system reaches a regime of statistical steady state in which the binary mixture is permanently driven away from equilibrium. (Fig. 20).

5.13 Viscous fingering with partially miscible fluids [5]

Viscous fingering—the fluid-mechanical instability that takes place when a low-viscosity fluid displaces a high-viscosity fluid—has traditionally been studied under either fully miscible or fully immiscible fluid systems. Here we study the impact of partial miscibility (a common occurrence in practice) on the fingering dynamics. Through a careful design of the thermodynamic free energy of a binary mixture, we develop a phase-field model of fluid-fluid displacements in a Hele-Shaw cell for the general case in which the two fluids have limited (but nonzero) solubility into one another. We show, by means of high-resolution numerical simulations, that partial miscibility exerts a powerful control on the degree of fingering: fluid dissolution hinders fingering while fluid exsolution enhances fingering (Fig. 21). We also show that, as a result of the interplay between compositional exchange and the hydrodynamic pattern-forming process, stronger fingering promotes that the system approach thermodynamic equilibrium faster.

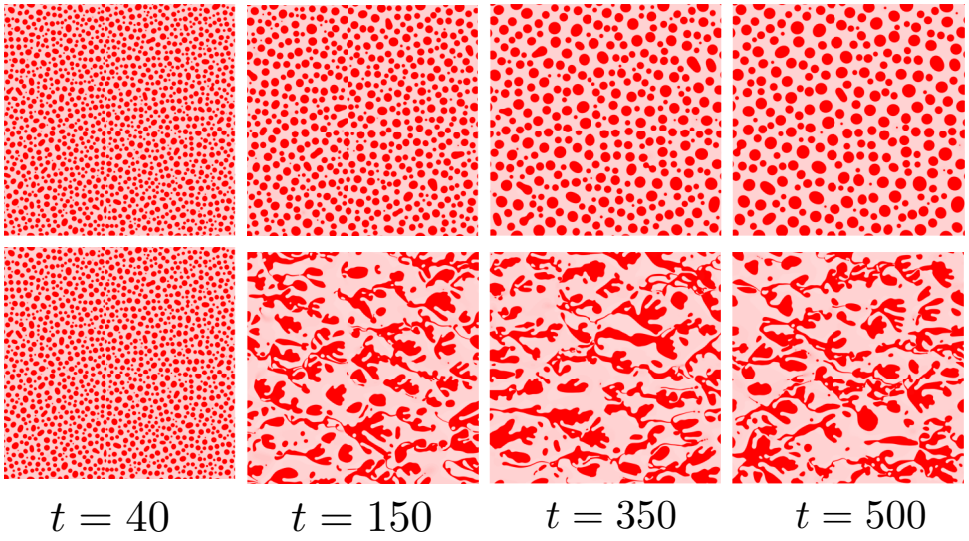

Figure 20. Snapshots of c at t=40, 150, 350 and 500, under no flow (top) and with periodic left-to-right flow imposed at t>40 (bottom).

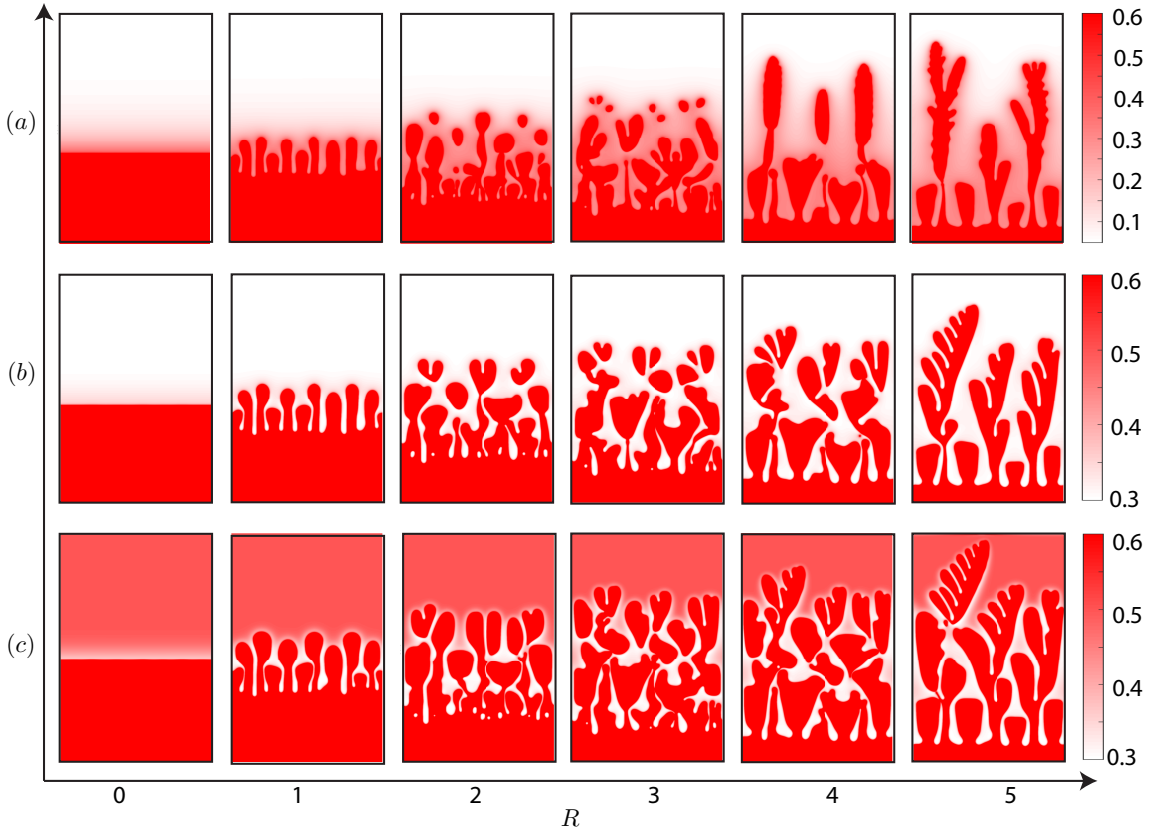

Figure 21. The coupling between different viscosity contrast and compositional effects lead to a rich set of viscous fingering patterns. Here we show snapshots of c at $t = 50$ for six different R values (across each row). Each of the three rows correspond to different c_l^0 values: defending liquid is (a) undersaturated; (b) near-saturated and (c) oversaturated. Note that the colormap differs between each row to reveal the detailed structures in the concentration field.

6 Conclusions

6.1 No geologic evidence that seismicity causes fault leakage that would render large-scale carbon capture and storage unsuccessful [11]

In a recent Perspective, Zoback and Gorelick (*Proc. Natl. Acad. Sci. USA* 109(26):1016410168, 2012) argued that carbon capture and storage (CCS) is likely not a viable strategy for reducing CO2 emissions to the atmosphere. They argued that maps of earthquake epicenters portray earthquakes occurring almost everywhere, suggesting that Earth's crust is near a critical state, so that increments in fluid pressure from injecting CO2 at 1 to 3 km depth will likely trigger earthquakes within the reservoir and caprock that would be expected to result in leakage of CO2 from the reservoirs to the surface.

Vast majority of earthquakes are much deeper than CO2 storage reservoirs. Zoback and Gorelick articulated an important, albeit well-known, concern: CCS may induce seismicity, as can other subsurface technologies. However, their characterization of seismic activity misrepresented its relevance to CCS. What is important is not epicenters (2D location on a map), but hypocenters (3D location, including depth). In fact, most hypocenters in the continental crust are in basement rock at 8 to 16 km depth, with only a very small fraction of them occurring in sedimentary cover at depths shallower than 3 km, where CO2 would be stored. The rheological properties of shallow sedimentary formations usually allow them to undergo substantial deformation without establishing leaking pathways or localized faults, in contrast with brittle basement rocks.

Hydrocarbon reservoirs have existed for millions of years in regions of intense seismic activity. Zoback and Gorelick stated that seismic activity would compromise containment of the CO2, and result in CO2 leakage to the surface. For justification, they referred to laboratory studies on granitic rocks—conditions that are not relevant for CCS. In reality, large volumes of buoyant fluids have remained stable in geologic traps over millennia in regions experiencing strong and frequent earthquakes, like southern California, even under substantial overpressures. If ubiquitous earthquake-induced leakage occurred, there would not be large quantities of natural gas still present in the subsurface.

Site selection is key. Although there are geologic settings in which induced earthquakes and leakage risk could compromise a CCS project (they mention the Mountaineer project), this says nothing about the many geologic formations that exhibit excellent promise for storing CO2. Zoback and Gorelick presented their conclusion that CCS will likely be unsuccessful without an analysis of the many suitable geologic formations available. In contrast, a recent study suggests that deep saline aquifers exist throughout the United States that can accommodate the CO2 migration and pressure increases associated with large-scale injection at the century time scale [16].

Summary. The facts that sedimentary cover rarely is the source region for earthquakes and that shallow overpressured hydrocarbon reservoirs coexist with deep basement seismicity do not support Zoback and Gorelick's conclusion that moderate-size earthquakes necessarily threaten seal integrity to the point of rendering CCS unsuccessful. We do not argue that the issues they raised are immaterial, but, rather, that more work on the physics of induced seismicity, fault activation, and geologic characterization in the context of CCS is needed.

7 Bibliography (Journal publications)

[1] D. Castineira, B. Jha, and R. Juanes. Uncertainty quantification and inverse modeling of fault poromechanics and induced seismicity: Application to a synthetic carbon capture and storage (CCS) problem. In *50th US Rock Mechanics Conference*, Houston, TX, June 26–29 2016.

[2] X. Fu, L. Cueto-Felgueroso, and R. Juanes. Pattern formation and coarsening dynamics in three-dimensional convective mixing in porous media. *Phil. Trans. R. Soc. A*, 371:20120355, doi:10.1098/rsta.2012.0355, 2013.

[3] X. Fu, L. Cueto-Felgueroso, D. Bolster, and R. Juanes. Rock dissolution patterns and geochemical shutdown of CO_2-brine-carbonate reactions during convective mixing in porous media. *J. Fluid Mech.*, 764:296–315, doi:10.1017/jfm.2014.647, 2015.

[4] X. Fu, L. Cueto-Felgueroso, and R. Juanes. Thermodynamic coarsening arrested by viscous fingering in partially-miscible binary mixtures. *Phys. Rev. E*, 94:033111, doi:10.1103/PhysRevE.94.033111, 2016.

[5] X. Fu, L. Cueto-Felgueroso, and R. Juanes. Viscous fingering with partially miscible fluids. *Phys. Rev. Fluids*, 2017. (Submitted).

[6] J. J. Hidalgo, J. Fe, L. Cueto-Felgueroso, and R. Juanes. Scaling of convective mixing in porous media. *Phys. Rev. Lett.*, 109:264503, doi:10.1103/PhysRevLett.109.264503, 2012.

[7] J. J. Hidalgo, C. W. MacMinn, and R. Juanes. Dynamics of convective dissolution from a migrating current of carbon dioxide. *Adv. Water Resour.*, 62:511–519, doi:10.1016/j.advwatres.2013.06.013, 2013.

[8] B. Jha and R. Juanes. Coupled modeling of multiphase flow and fault poromechanics during geologic CO_2 storage. *Energy Procedia* (Proc. GHGT-12), 63:3313–3329, 2014.

[9] B. Jha and R. Juanes. Coupled multiphase flow and poromechanics: a computational model of pore-pressure effects on fault slip and earthquake triggering. *Water Resour. Res.*, 50(5): 3776–3808, doi:10.1002/2013WR015175, 2014.

[10] B. Jha, F. Bottazzi, R. Wojcik, M. Coccia, N. Bechor, D. McLaughlin, T. A. Herring, B. H. Hager, S. Mantica, and R. Juanes. Reservoir characterization in an underground gas storage field using joint inversion of flow and geodetic data. *Int. J. Numer. Anal. Methods Geomech.*, 39(4):1619–1638, doi:10.1002/nag.2427, 2015.

[11] R. Juanes, B. H. Hager, and H. J. Herzog. No geologic evidence that seismicity causes fault leakage that would render large-scale carbon capture and storage unsuccessful. *Proc. Natl. Acad. Sci. U.S.A.*, 109(52):E3623, 2012.

[12] R. Juanes, B. Jha, B. H. Hager, J. H. Shaw, A. Plesch, L. Astiz, J. H. Dieterich, and C. Frohlich. Were the May 2012 Emilia–Romagna earthquakes induced? A coupled flow-geomechanics modeling assessment. *Geophys. Res. Lett.*, 43(13):6891–6897, doi:10.1002/2016GL069284, 2016.

[13] J. Kim, H. A. Tchelepi, and R. Juanes. Rigorous coupling of geomechanics and multiphase flow with strong capillarity. *Soc. Pet. Eng. J.*, 18(6):1123–1139, doi:10.2118/141268–PA, 2013.

[14] C. W. MacMinn and R. Juanes. Buoyant currents arrested by convective dissolution. *Geophys. Res. Lett.*, 40:2017–2022, doi:10.1002/grl.50473, 2013.

[15] M. L. Szulczewski and R. Juanes. The evolution of miscible gravity currents in horizontal porous layers. *J. Fluid Mech.*, 719:82–96, doi:10.1017/jfm.2012.631, 2013.

[16] M. L. Szulczewski, C. W. MacMinn, H. J. Herzog, and R. Juanes. Lifetime of carbon capture and storage as a climate-change mitigation technology. *Proc. Natl. Acad. Sci. U.S.A.*, 109 (14):5185–5189, doi:10.1073/pnas.1115347109, 2012.

[17] M. L. Szulczewski, M. A. Hesse, and R. Juanes. Carbon dioxide dissolution in structural and stratigraphic traps. *J. Fluid Mech.*, 736:287–315, doi:10.1017/jfm.2013.511, 2013.

[18] M. L. Szulczewski, C. W. MacMinn, and R. Juanes. Theoretical analysis of how pressure buildup and CO_2 migration can both constrain storage capacity in deep saline aquifers. *Int. J. Greenh. Gas Control*, 23:113–118, doi:10.1017/jfm.2014.512, 2014.

[19] Y. Tal and B. H. Hager. An empirical study of the distribution of earthquakes with respect to rock type and depth. *Geophys. Res. Lett.*, 42(18):7406–7413, 2015.

[20] Z. Yang and R. Juanes. The two sides of a fault: grain-scale analysis of fault slip under discontinuous pore pressure. *Geophys. Res. Lett.*, 2017. (Submitted).

[21] B. Zhao, C. W. MacMinn, M. L. Szulczewski, J. A. Neufeld, H. E. Huppert, and R. Juanes. Interface pinning of immiscible gravity-exchange flows in porous media. *Phys. Rev. E*, 87: 023015, doi:10.1103/PhysRevE.87.023015, 2013.

[22] B. Zhao, C. W. MacMinn, H. E. Huppert, and R. Juanes. Capillary pinning and blunting of immiscible gravity currents in porous media. *Water Resour. Res.*, 50(9):7067–7081, doi:10.1002/2014WR015335, 2014.

[23] B. Zhao, C. W. MacMinn, and R. Juanes. Residual trapping, solubility trapping and capillary pinning complement each other to limit CO2 migration in deep saline aquifers. *Energy Procedia* (Proc. GHGT-12), 63:3833–3839, 2014.

8 Appendix: Selected invited lectures and talks

07/2016 Frontiers of Geoscience Colloquium, Computational modeling of induced seismicity, Los Alamos National Laboratory, Los Alamos, NM.

06/2016 Plenary speaker, Computational modeling of induced seismicity, Computational Methods in Water Resources Conference — CMWR 2016, Toronto

02/2016 Computational modeling of induced seismicity, Harvard University, Cambridge, MA

11/2015 Computational modeling of induced seismicity, Northeastern University, Boston, MA

09/2015 Plenary keynote speaker, Computational modeling of induced seismicity, TOUGH Symposium, Lawrence Berkeley National Lab, Berkeley, CA.

07/2015 Invited lecture, Cargése Summer School on Flow and Transport in Porous and Fractured Media, Corsica, France.

06/2015 Plenary lecture, Computational modeling of induced seismicity, Engineering Mechanics Institute Conference — EMI 2015, Stanford.

05/2015 Invited talk, Computational modeling of coupled multiphase flow and geomechanics to study fault slip and induced seismicity, SIAM Geosciences Conference, Stanford.

04/2015 Computational modeling of coupled multiphase flow and geomechanics to study fault slip and induced seismicity, Penn State University.

01/2015 Computational modeling of coupled multiphase flow and geomechanics to study fault slip and induced seismicity, Department of Geophysics, Stanford University.

01/2015 Computational modeling of coupled multiphase flow and geomechanics to study fault slip and induced seismicity, Lawrence Livermore National Laboratory.

12/2014 Invited talk, A Computational Model of Coupled Multiphase Flow and Geomechanics to Study Fault Slip and Induced Seismicity, AGU Fall Meeting, San Francisco, CA.

11/2013 Lifetime of carbon capture and storage as a climate change mitigation technology, MIT-Total Symposium, Cambridge, MA.

06/2013 Invited talk, Lifetime of carbon capture and storage as a climate change mitigation technology, SIAM Geosciences Conference, Padova, Italy.

01/2013 Invited lecture, Lifetime of carbon capture and storage as a climate change mitigation technology, Fermilab Colloquium, Fermi National Accelerator Laboratory, IL.